

Selective and Ratiometric Fluorescent Trapping and Quantification of Protein Vicinal Dithiols and in Situ Dynamic Tracing in Living Cells

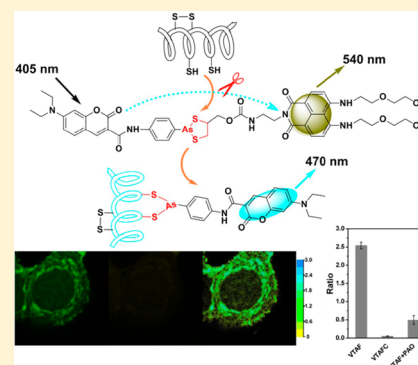
Chusen Huang,^{†,‡} Ti Jia,[‡] Mengfang Tang,[†] Qin Yin,[†] Weiping Zhu,^{*,†} Chao Zhang,[†] Yi Yang,[†] Nengqin Jia,^{*,‡} Yufang Xu,^{*,†} and Xuhong Qian[†]

[†]State Key Laboratory of Bioreactor Engineering, Shanghai Key Laboratory of Chemical Biology, School of Pharmacy, East China University of Science and Technology, 130 Meilong Road, Shanghai 200237, China

[‡]The Education Ministry Key Laboratory of Resource Chemistry and Shanghai Key Laboratory of Rare Earth Functional Materials, Department of Chemistry, College of Life and Environmental Sciences, Shanghai Normal University, 100 Guilin Road, Shanghai 200234, China

S Supporting Information

ABSTRACT: Protein vicinal dithiols play fundamental roles in intracellular redox homeostasis due to their involvement in protein synthesis and function through the reversible vicinal dithiol oxidation to disulfide. To provide quantitative information about the global distribution and dynamic changes of protein vicinal dithiols in living cells, we have designed and synthesized a ratiometric fluorescent probe (VTAF) for trapping of vicinal dithiol-containing proteins (VDPs) in living cells. VTAF exhibits a ratiometric fluorescence signal upon single excitation, which enables self-calibration of the fluorescence signal and quantification of endogenous vicinal dithiols of VDPs. Its potential for in situ dynamic tracing of changes of protein vicinal dithiols under different cellular redox conditions was exemplified. VTAF facilitated the direct observation of subcellular distribution of endogenous VDPs via ratiometric fluorescence imaging and colocalization assay. And the results suggested that there are abundant VDPs in mitochondria. Moreover, some redox-sensitive VDPs are also present on cell surface which can respond to redox stimulus. This ratiometric fluorescence technique presents an important extension to previous fluorescence intensity-based probes for trapping and quantifying protein vicinal dithiols in living cells, as well as its visible dynamic tracing of VDPs.



INTRODUCTION

Redox-based post-translational modification of protein thiols plays fundamental roles in cellular homeostasis and cell signaling,^{1–4} and reversible protein vicinal dithiol oxidation to disulfide holds a particularly prominent position due to its involvements in protein synthesis and function, and implications in cancer,^{5,6} diabetes,⁷ platelet function,⁸ human immunodeficiency virus type 1 (HIV-1),^{9–11} neurodegeneration,¹² and so forth. Apart from its special role as the redox center, the protein vicinal dithiols are also a key linking center for formation and stabilization of protein structures during the protein post-translational modification, which is considered to be closely related to protein functions.^{13–16} Therefore, trapping and identifying cellular protein vicinal dithiols levels are valuable not only for further investigation of the protein post-translational modifications, but also for the redox related disease diagnosis and pathophysiology elucidation.¹⁷

Since trivalent arsenicals can selectively interact with protein vicinal dithiols, *p*-aminophenylarsenoxide (PAO) and thiol alkylation agents have been widely used to estimate different concentrations of monothiol and total thiol groups through selective labeling of vicinal dithiols with PAO, then the protein vicinal dithiols can be quantified by another thiol alkylation agent after removal of PAO.¹⁸ This common

approach has identified some new vicinal dithiol-containing proteins (VDPs) in cell lysate. Additionally, arsenite (III)-affinity chromatography,^{19–21} biotinylated conjugates of PAO,^{22,23} and dimaleimide fluorogens have also been introduced to make the proteomic study of VDPs with different possible functions (Supporting Information Scheme S1). However, these methods focused on developing strategies for unveiling VDPs in cell lysate and cannot collect more information about the global distribution and dynamic changes of endogenous VDPs *in situ*. Thus, in order to investigate the essential roles of protein vicinal dithiols in cellular redox homeostasis and protein function in living cells, the vicinal dithiols of VDPs should be specifically labeled and trapped ideally in living cells prior to cell lysate.²⁴

Previously, we developed a highly selective fluorescent probe (NPE) based on 2-*p*-aminophenyl-1,3,2-dithiarsenolane (VTA2) and naphthalimide, which could enable an *in situ* imaging of VDPs through the direct fluorescence readout.²⁵ Most recently, a monoarsenical fluorescent probe (TRAP_Cy3) based on cyanine chromophore has also been exploited to identify that protein vicinal dithiols can decrease

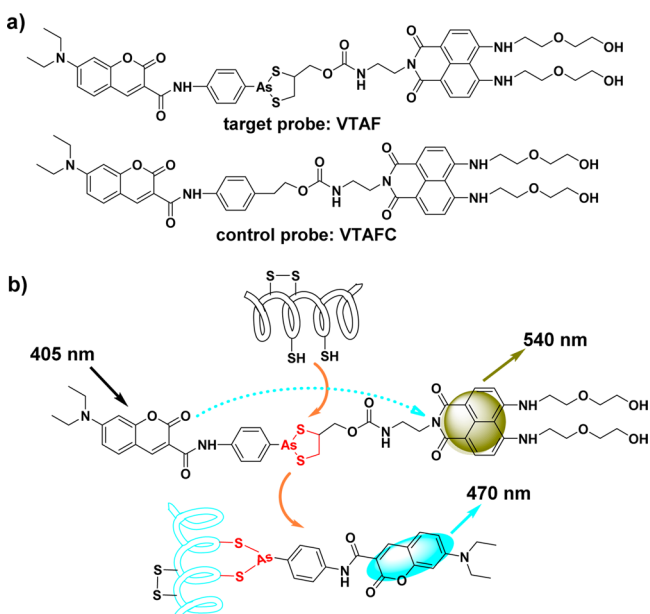
Received: August 4, 2014

Published: September 15, 2014

oxidative protein damage in adaptive microbial responses.²⁶ TRAP_Cy3 and NPE can trace the redox response of protein vicinal dithiols within living cells. However, a potential drawback of these chemical probes is the background fluorescence from unreacted or nonspecifically bound probes. A long washing procedure (at least 15 min) is needed to remove the unbound probes in order to reduce the fluorescence background, which might make measurements prone to artifacts. Moreover, although the endogenous VDPs have been visualized by labeled fluorescent probes, the fluorescence-intensity based signal may be obstructed by the probe's concentration, inhomogeneous cellular distribution, variations in excitation intensity, sample thickness, and other environment factors such as changes in pH and temperature, thus diminishing its capacity to provide more accurate and quantitative information about dynamic changes of vicinal dithiols on VDPs in living cells. Comparatively, ratiometric fluorescent probes are of considerable practical value for reducing the influence of above factors since the detectable signal can be reflected through the ratio of emission intensity at two wavelengths.^{27–31}

Herein, we report a ratiometric fluorescent probe (VTAF) based on fluorescence resonance energy transfer (FRET) mechanism for endogenous VDPs and exemplify its potentials for imaging protein vicinal dithiols in *in vitro* studies. VTAF exhibits a ratiometric fluorescence signal upon single excitation, which enables self-calibration of the fluorescence signal and quantification of endogenous vicinal dithiols of VDPs within live cells. As a result, the VDPs are specifically labeled by a coumarin fluorophore after their interaction with VTAF. Because the emissions of VTAF and fluorescently labeled VDPs are different, unreacted VTAF does not need to be washed out (Scheme 1). To our knowledge, VTAF is the first ratiometric fluorescent probe for trapping endogenous VDPs in live cells.

Scheme 1. (a) Chemical Structures of VTAF and VTAF1; (b) Design Strategy of VTAF for Selective and Ratiometric Measurements of VDPs



RESULTS AND DISCUSSION

Design and Synthesis of VTAF. Our investigation begins with design and synthesis of a selective and ratiometric VDPs-responsive fluorescent probe based on FRET mechanism. We have previously synthesized a highly selective receptor (2-*p*-aminophenyl-1,3,2-dithiarsenolane (VTA2)) for VDPs based on the specific interaction of trivalent arsenic with protein vicinal dithiols, while monothiol of protein have much lower affinity.³² VTA2 displayed high stability and biocompatibility (higher cell permeability and lower toxicity) compared to PAO through introduction of a 1,2-ethanedithiol on the structure of PAO.^{25,33} We envisioned that a FRET platform was constructed by combining two fluorophores to the trivalent arsenic based receptor with similar structure to VTA2. These two fluorophores were the energy donor and acceptor of a FRET pair. Thus, we designed the target probe VTAF (Scheme 1), which bears a coumarin and a naphthalimide for signal transduction, and the aforementioned arsenic moiety (VTAF1, Supporting Information Scheme S2) for selective interaction with VDPs. When excited at 405 nm, the FRET will move from the coumarin to the naphthalimide. After vicinal dithiols on VDPs selectively interchange with 2,3-dimercaptopropanol moiety of VTAF, two fluorophores are no longer in proximity, which is essential for efficiency, and hence, FRET is prohibited (Scheme 1). Thus, the ratiometric signal will be related to VDPs. Meanwhile, VDPs will also be specifically labeled by coumarin moiety, which will make the *in situ* tracing and further proteomic study of VDPs possible. As the fluorescence signal of coumarin moiety was released after the VDPs were specifically labeled by VTAF, a wash-out of the unreacted probe is no longer necessary.

The synthetic route for preparing VTAF was depicted in Supporting Information Scheme S2. First, protecting group 2,3-dimercaptopropanol was introduced into PAO to furnish VTAF1, which was further modified by coumarin (FRET donor) and 1,8-naphthalimide (FRET acceptor). The integration of two diglycol amine groups at 4,5-position of 1,8-naphthalimide can tune the hydrophilicity and lipophilicity of VTAF, which enables both the water solubility and cell-permeability of the probe. VTAF was synthesized in nine steps under mild conditions. Similarly, a control probe without trivalent arsenic group (VTAF1, Scheme 1a) was also synthesized (Supporting Information Scheme S3).

Spectroscopic Properties and Optical Responses to VDPs. A pH titration was conducted. As displayed by the emission at 540 and 470 nm, respectively, negligible fluorescence changes were observed during the pH range of 6–10 (Supporting Information Figure S1). Thus, a PBS buffer (10 mM PBS, 5 mM EDTA, pH 7.4, 0.5% DMSO) was chosen as the test medium in the molecular level assay. Meanwhile, a stability test for VTAF in PBS buffer was also conducted to check whether the urethane group of VTAF will be hydrolyzed by water at neutral pH. As shown in Supporting Information Figure S2, no fluorescence changes were observed, which indicated that VTAF was not hydrolyzed even after 3 h. Next, the fluorescence response of VTAF toward VDPs was tested. Reduced bovine serum albumin (rBSA) was taken as the model VDPs. There were about 17 pairs of vicinal thiols in rBSA after the BSA was treated with reducing agent dithiothreitol (DTT). As shown in Figure 1a, upon addition of 1 equiv amount of rBSA, fluorescence emission centered at 470 nm increased

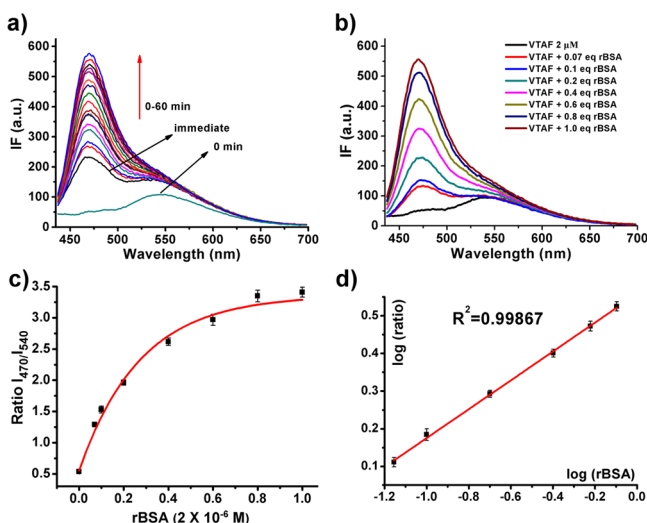


Figure 1. (A) Time-dependent fluorescence response of VTAF (2 μM) to 1 equiv rBSA (2 μM) in PBS buffer. (B) Ratiometric fluorescence response of VTAF (2 μM) to different concentrations of rBSA in PBS buffer. (C) Ratiometric determination of rBSA by calculation of ratio of emission intensity at 470 and 540 nm. (D) Linear relationship between ratio and concentration of rBSA (from 0.14 to 1.6 μM). $\lambda_{\text{ex}} = 405 \text{ nm}$. Error bars (SD) represent three independent experiments; $\log(\text{ratio}) = \log(\text{ratio } I_{470}/I_{540})$, rBSA = reduced BSA (with vicinal dithiols).

remarkably with a concomitant minor increase of fluorescence emission at 540 nm under the excitation wavelength at 405 nm. It was observed that the fluorescence intensity changed immediately and then reached a plateau within 60 min. This result demonstrates that VTAF interacts with rBSA very fast in the beginning, and then reached equilibrium. Control probe VTAFc was also applied for the interaction with rBSA. As suggested in Supporting Information Figure S3, negligible changes in the fluorescence signal were observed in the presence of 1 equiv of rBSA, even the reaction time extended to 60 min. These results indicated that the trivalent arsenic moiety of VTAF was needed for its selective interaction with VDPs. In the following molecular-based assays, the detection was allowed to react for 60 min. To test the sensitivity of VTAF for rBSA, the changes in fluorescence emission were recorded upon gradual addition of rBSA (from 0 to 2 μM). Excitation at 405 nm produces a fluorescence spectrum featuring one dominant emission band centered at 470 nm (Figure 1b). When the amount of rBSA increased to 2 μM , fluorescence changes at 470 nm reached a plateau, which can be directly reflected by the fluorescence ratio of emission at 470 and 540 nm (ratio I_{470}/I_{540} , Figure 1c). From the concentration-dependent ratio changes, the detection limit of VTAF for rBSA was determined to be 0.14 μM . Then, we take the logarithm of ratio I_{470}/I_{540} and concentration of rBSA, which was defined as $\log(\text{ratio } I_{470}/I_{540})$ and $\log(\text{rBSA})$, respectively. Through a linear regression by Origin 8.0 software, a linear relationship between $\log(\text{ratio } I_{470}/I_{540})$ and $\log(\text{rBSA})$ was observed (Figure 1d). Hence, a linear relationship between changes of ratio I_{470}/I_{540} and the concentrations of rBSA (changes from 0.14 to 1.6 μM , Figure 1c,d) can be deduced. The obtained linear curve makes quantitative detection of rBSA very convenient over this concentration range. This also presents a platform for quantitative determination of VDPs by using VTAF.

To test whether other biological analytes could interfere with this detection, fluorescence responses of VTAF for some small amino acids (or peptide) were also studied. As shown in Figure 2a, no significant fluorescence changes of VTAF were

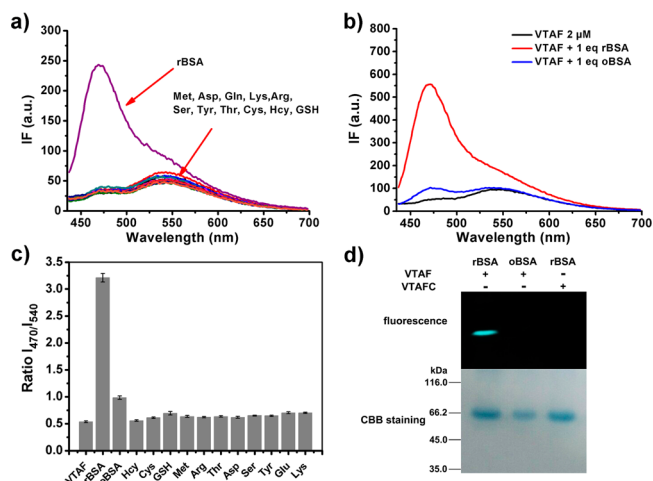


Figure 2. Selectivity of VTAF to rBSA. (A) Changes in fluorescence emission spectra of VTAF (1 μM) with addition of rBSA (1 μM) and other small amino acids (100 μM) after 60 min in PBS buffer. (B) Changes in fluorescence emission of VTAF (2 μM) with addition of rBSA (2 μM) and oBSA (2 μM). (C) Ratio changes in fluorescence intensity (based on the peak heights at the maxima, 470 and 540 nm, respectively) with addition of rBSA and other interfering reagents after 60 min. $\lambda_{\text{ex}} = 405 \text{ nm}$. Error bars (SD) represent three independent experiments. (D) Selectivity of VTAF to VDPs was identified by SDS-PAGE. rBSA = reduced BSA (with vicinal dithiols), oBSA = oxidized BSA (without vicinal dithiols).

observed in the presence of 100-fold amounts of different common amino acids (or peptide) such as cysteine (Cys), homocysteine (Hcy), glutathione (GSH), etc. In contrast, upon addition of 1 equiv of rBSA, a blue shift of about 70 nm can be observed. Similarly, 1 equiv of oxidized BSA (oBSA, which was treated with hydrogen peroxide as an oxidant to remove vicinal dithiols on BSA) also induced negligible fluorescence changes of VTAF (Figure 2b). These results can be recorded by the ratio changes of fluorescence intensity (Ratio I_{470}/I_{540} , Figure 2c), from which the high selectivity of VTAF to rBSA can be clearly observed. The ratio of fluorescence intensities at 470 and 540 nm varies from 0.5 (in the absence of rBSA) to 3.2 (in the presence of rBSA) with a 6-fold increase. Other common biological analytes (even the concentration was 100-fold excess over VTAF) exhibited no discernible ratio changes. Specifically, the ratiometric sensing of rBSA is unperturbed by the varied concentrations of VTAF (Supporting Information Figure S4). These data demonstrated that VTAF represents a more accurate probe for determination of VDPs through the ratiometric signals. Meanwhile, electrophoresis studies were also carried out to further identify the high selectivity of VTAF to VDPs. A fluorescent band was observed only in the lane loaded with rBSA and VTAF, whereas the lane loaded with oBSA and VTAF exhibited no fluorescence signal. Coomassie Brilliant Blue (CBB) staining demonstrated that the fluorescent band was related to the formations of rBSA–probe complex (Figure 2d). There was no fluorescent band observed when VTAFc, which lacks of the cyclic dithiaarsane moiety, was used for labeling. These results indicated that the

cyclic dithiaarsane moiety in VTAF was cleaved by vicinal dithiols of rBSA, and the coumarin moiety was attached to rBSA through the interaction of vicinal dithiols of rBSA with trivalent arsenic of coumarin moiety (Scheme 1). All these results demonstrated that VTAF was a highly selective fluorescent probe for VDPs.

In Situ Imaging of Endogenous VDPs with VTAF in Live Cells. We then explored whether VTAF could be used to detect the endogenous VDPs in live cells. Previously, some different VDPs have been unveiled in MCF-7 cells, and these VDPs are found to be related with redox regulation.³⁴ Thus, we performed the ratiometric imaging of endogenous VDPs in living MCF-7 cells by confocal microscopy. Initially, the cytotoxicity of VTAF was tested by MTT assay. As demonstrated in Supporting Information Figure S5, above 90% of MCF-7 cells survived after the cells were incubated with 5 μM of VTAF for 12 h, and after 24 h, the cell viability remained at 85%, which indicated the very low cytotoxicity of VTAF when it was used in 5 μM . Thus, concentration of VTAF was taken as 5 μM for the next cell imaging experiments. Then incubation of MCF-7 with VTAF at 5 μM was conducted for 30 min at 37 $^{\circ}\text{C}$. The fluorescence signal was collected before removal of extracellular free VTAF. Upon excitation by 405 nm laser line, a strong fluorescence signal at coumarin channel (emission signal was collected at 450–490 nm) and a relatively weak fluorescence signal at naphthalimide channel (emission signal was collected at 530–590 nm) were observed (Figure 3a, top). When VTAF was

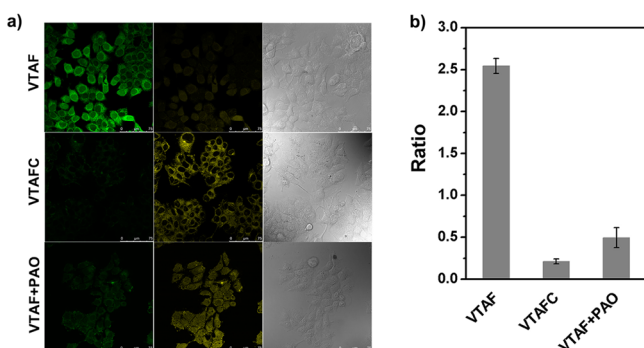


Figure 3. (A) In situ fluorescence imaging of cellular VDPs in MCF-7 cells. VTAF and VTAF+PAO: Cells were treated with 5 μM of VTAF and VTAF+PAO, respectively. VTAF + PAO: VTAF was coincubated with 25 μM PAO in cells. Fluorescence was collected at coumarin channel, 450–490 nm (left, green); naphthalimide channel, 530–590 nm (middle, yellow) upon excitation by 405 nm laser line. Scale bar, 75 μm . (B) Semiquantitative determination of endogenous VDPs in MCF-7 cells according to the ratio of averaged fluorescence intensity of coumarin channel (450–490 nm) to naphthalimide channel (530–590 nm). The semiquantitative calculation was conducted by ImageJ software. Error bars represent SD.

coincubated with PAO at 25 μM in live cells, the fluorescence signal at coumarin channel decreased with the increase of fluorescence signal at naphthalimide channel (Figure 3a, middle). Treatment of cells with VTAF+PAO (5 μM) leads to negligible fluorescence signal at coumarin channel and strong fluorescence signal at naphthalimide channel (Figure 3a, bottom). The semiquantitative calculation of ratio of coumarin channel to naphthalimide channel at averaged emission intensity was further conducted. As suggested in Figure 3b, the high ratio for VTAF-loaded cells indicates that

MCF-7 cells contain a high level of VDPs. An approximately 5-fold decrease in ratio for cells treated with VTAF and PAO was observed, which reveals that the labeling of cellular VDPs was inhibited by PAO through the competitive binding of PAO with vicinal dithiols on VDPs. The ratio of cells treated with VTAF+PAO was about 0.21, which is approximately 12-fold decrease compared to the VTAF-loaded cells. These results demonstrated that VTAF was a highly selective and effective tool for ratiometric trapping of endogenous VDPs in live cells.

In the case of protein labeling in live cells, many developed labeling technologies based on synthetic small fluorescent probes need a “washout” procedure to remove intracellular free probes. Herein, VTAF can specifically label endogenous VDPs without long-time washing procedure. In the specific protocol, cells were incubated with VTAF in a fresh medium (serum-free DMEM) for 30 min. After the culture medium was replaced with fresh PBS to remove extracellular free VTAF, cell images were conducted under confocal microscopy immediately. A clear strong fluorescence signal at coumarin channel and a relatively weak fluorescence signal at naphthalimide channel were observed (Supporting Information Figure S6, Bottom). In addition, the procedure for replacing culture medium with fresh PBS is applied to remove extracellular free VTAF, which will make the semiquantitative determination of averaged fluorescence intensity at naphthalimide channel more accurate. As indicated in Supporting Information Figure S6 (top), before the culture medium was replaced with fresh PBS, there were no changes in the fluorescence signal from cells at both coumarin and naphthalimide channel except that some extracellular yellow spots were removed, which will be beneficial for ratiometric quantitative determination of endogenous VDPs in live cells. Accordingly, VTAF can specifically label endogenous VDPs in live cells without long-time washing procedure. Additionally, live cells were incubated with VTAF in a fresh medium (serum-free DMEM) without wash procedure, then the cell imaging of endogenous VDPs was conducted directly under confocal microscopy for continuous observation of fluorescence signal at both coumarin channel and naphthalimide channel at the time point of 30, 45, and 60 min, respectively. As shown in Supporting Information Figure S7, the fluorescence signal at both coumarin channel and naphthalimide channel did not change at the time of 30, 45, and 60 min, respectively. Especially for the fluorescence signal at naphthalimide channel, there is no increase in the extracellular fluorescence intensity. Similarly, no loss of intracellular fluorescence intensity was observed at the naphthalimide channel. Thus, this result demonstrated that the naphthalimide unit might not be excluded by cells after the naphthalimide unit leaves from the coumarin units in VTAF. And the cellular concentration of naphthalimide unit did not change after the interaction of VTAF with VDPs, which could enable an accurate semiquantitative analysis in live cells. Through the semiquantitative calculation, there was no significant difference in the ratio at the time point of 30 and 60 min, respectively (Supporting Information Figure S8). This result confirmed that the interaction between VTAF and endogenous VDPs in live cells is completed in 30 min. Compared to the relatively slow response time of VTAF to rBSA (about 1 h), we deduced that the interaction between VTAF and VDPs is a dynamic equilibrium (please see the detailed discussion in the Supporting Information).

Dynamic Tracing of Endogenous VDPs with VTAF in Live Cells. The successful use of VTAF for trapping of endogenous VDPs prompted us to apply this probe for the monitoring of dynamic changes of VDPs under a redox stimulus in living cells. Diamide is a commonly used thiol oxidant that can oxidize protein vicinal thiols to disulfide.³⁵ After VTAF and diamide were coincubated in MCF-7 cells, the fluorescence intensity at coumarin channel decreased and an increase in fluorescence intensity at naphthalimide channel was observed (Figure 4a, VTAF+Diamide). Semiquantitative

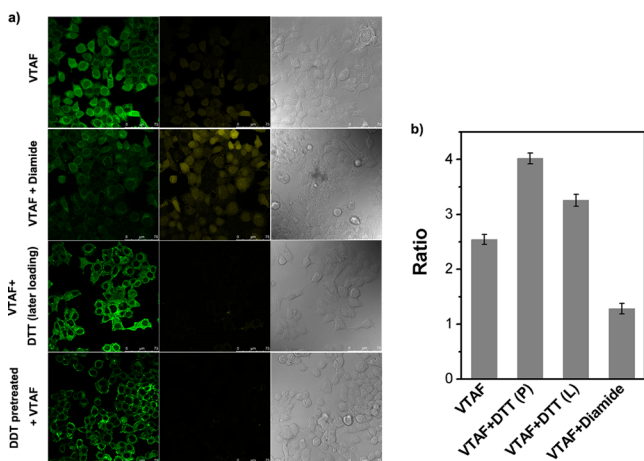


Figure 4. Dynamic tracing of VDPs under redox reagents stimulus in live cells according to ratiometric fluorescence change (coumarin channel (450–490 nm)/naphthalimide channel (530–590 nm)). (A) Ratiometric fluorescence imaging of VDPs in live cells. Excitation wavelength: 405 nm. Emission collection: coumarin channel, 450–490 nm (left, green); naphthalimide channel, 530–590 nm (middle, yellow). Scale bar, 75 μm . (B) Semiquantitative determination of endogenous VDPs in MCF-7 cells according to ratio of averaged fluorescence intensity at coumarin channel (450–490 nm) and naphthalimide channel (530–590 nm). VTAF, VTAF + Diamide: cells loaded with VTAF, VTAF and Diamide, respectively. VTAF + DTT (P): cells pretreated with DTT (10 mM) for 10 min, then loaded with VTAF. VTAF + DTT (L): cells loaded with VTAF first and incubation for 10 min, then DTT was loaded. VTAF (5 μM), DTT (10 mM), and Diamide (50 μM) were used in these experiments. Error bars represent SD.

determination clearly demonstrated that about 1.8-fold decrease in ratios of fluorescence intensity was observed, compared to no diamide treated cells (Figure 4b, VTAF + Diamide), which indicated that levels of protein vicinal thiols decreased owing to the formation of disulfide under the oxidant stimulus. Similarly, cells were loaded with 5 μM VTAF, followed by exposure to 10 mM DTT 10 min later. After incubation for another 20 min, the fluorescence signal at coumarin channel was a little brighter and fluorescence intensity at naphthalimide channel decreased to baseline levels (Figure 4a, VTAF + DTT (later loading)). The observed ratio increase was about 1.3-fold compared to DTT untreated cells (Figure 4b, VTAF + DTT (L)). These data demonstrated that VTAF can trace the changes of VDPs under different cellular redox states. Thus, VTAF can be applied for identifying and studying the levels of cellular protein vicinal dithiols that play key roles in cellular redox homeostasis, which is of considerable significance for both VDPs related disease diagnosis and exploration of its diverse pathophysiology.

Through the plot analysis of regions of interest (ROI) across MCF-7 cells, it is noteworthy that the MCF-7 cell membrane exhibited brighter fluorescence at coumarin channel when the cells were loaded with 5 μM VTAF, followed by exposure to 10 mM DTT 10 min later (Figure 5b), which may indicate an increase in levels of protein vicinal

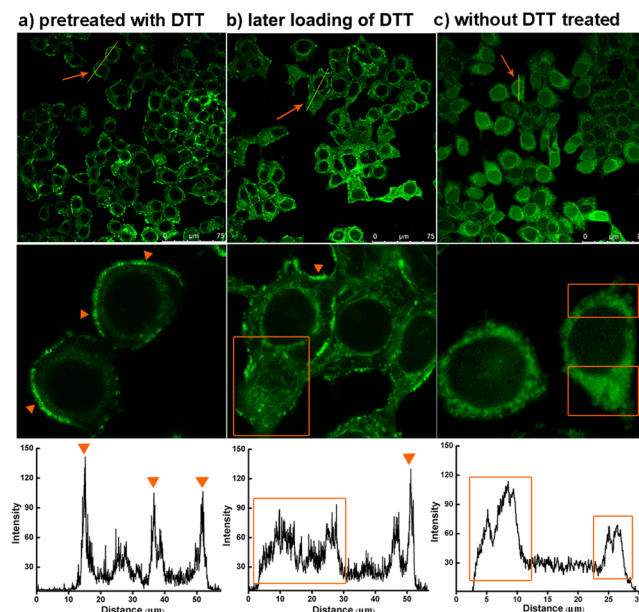


Figure 5. Top: Fluorescence imaging of live cells with VTAF. Scale bar 75 μm . Middle: Plot analysis of regions of interest (ROI) across MCF-7 cells. Excitation wavelength: 405 nm. Emission collection: 450–490 nm (coumarin channel). Bottom: Intensity profile of linear ROI across MCF-7 cells. ROI was conducted by ImageJ software. Pretreated with DTT: cells pretreated with DTT (10 mM) for 10 min, then loaded with VTAF. Later loading of DTT: cells loaded with VTAF first and incubation for 10 min, then DTT was loaded. VTAF (5 μM) and DTT (10 mM) were used in these experiments.

dithiols in cell membrane. To further investigate whether there is an increase in levels of protein vicinal thiols in living cell membrane under reductant stimulus, the cells were preincubated with 10 mM DTT for 10 min, then 5 μM VTAF was loaded and incubated for another 20 min. As suggested in Figure 4a (DTT pretreated + VTAF) and Figure 5a (pretreated with DTT), fluorescence signal at coumarin channel increased along the cell membranes while the cytoplasm exhibited very weak fluorescence signal compared to DTT-untreated cells (Figure 5c). A comparison of enlarged images based on plot analysis of ROI and intensity profile of linear ROI across MCF-7 cells (Figure 5, middle and bottom) further demonstrated that fluorescence signal on MCF-7 cell membranes increased under DTT stimulus. Similarly, the ratio value of coumarin channel/naphthalimide channel also increased to about 4.0 (Figure 4b, VTAF + DTT (P)), which was 1.6-fold compared to DTT untreated cells. This result displayed an interesting phenomenon and we speculated that DTT pretreatment makes some more redox-sensitive protein disulfides on cell surface become protein vicinal dithiols that can be specifically labeled and visualized by VTAF. This hypothesis can be partially supported by previous study that reveals the existence of some redox active protein vicinal dithiols on cell surface.³⁶ This interaction between redox-sensitive cell-surface protein vicinal dithiols and VTAF

hinders the probe's penetration into cells. Then only a little VTAF enters the cytoplasm and intracellular VDPs are visualized. Through the plot analysis of ROI across MCF-7 cells (Figure 5), we can conclude that reductant stimulation leads to an increase in levels of endogenous protein vicinal dithiols in MCF-7 cells. Moreover, some redox-sensitive VDPs are present on cell surface which may regulate the function of live cells through the reversible protein vicinal dithiols oxidation to disulfides.

Subcellular Distribution Study of Intracellular VDPs and Ratiometric Images with VTAF. We have previously studied the subcellular distribution of intracellular VDPs in Chang liver cells.²⁵ Herein, the localization of intracellular VDPs was also investigated in live MCF-7 cells. With the use of confocal microscopy, the fluorescence signal at coumarin channel displayed a punctuated pattern mainly concentrated in a small, eccentric perinuclear zone (Figure 6, VTAF;

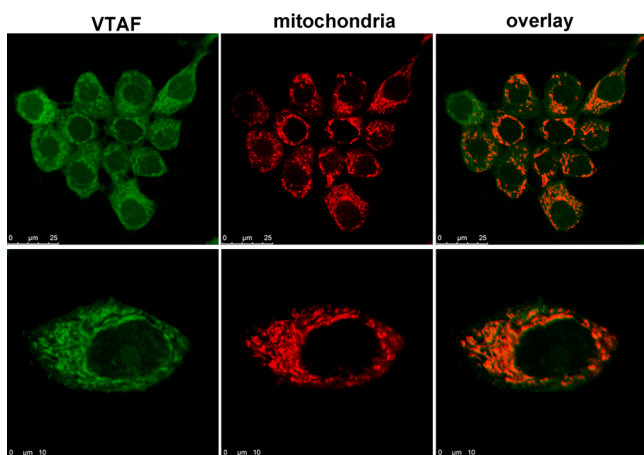


Figure 6. Top: Colocalization of VTAF (5 μM) with Mito-Tracker Deep Red (50 nM) in live MCF-7 cells. Scale bar 25 μm . Bottom: enlarged images of single cell stained with VTAF and Mito-Tracker Deep Red. Scale bar 10 μm . Excitation wavelength for VTAF: 405 nm. Emission collection: coumarin channel, 450–490 nm (VTAF, green). The excitation of Mito-Tracker Deep red is 633 nm, and >650 nm emission light was collected (mitochondria, red). Overlay: the merged images of VTAF and mitochondria (overlay, orange). Pearson's correlation coefficient of 0.86 ± 0.04 was obtained by using the JACoP plugin on ImageJ and Image-Pro Plus (IPP 6.0) software.

Supporting Information Figures S6A and S9A). Meanwhile, the fluorescence signal in cytoplasm matrix and nucleus was scarcely observed. By contrast, the weak fluorescence signal at naphthalimide channel showed a wide pattern in cells (Supporting Information Figures S6B and S9B). These results confirmed that the fluorescence signal in punctuated pattern was mainly from labeled VDPs. And the punctuated pattern indicated a mitochondrial localization. Then a colocalization assay was conducted through the coinubation of Mito-Tracker Deep Red (a commercial probe for specific staining of mitochondria) with VTAF in live MCF-7 cells. As depicted in Figure 6, mitochondria were stained by Mito-Tracker Deep Red and exhibited clear fluorescence signal at red channel (>650 nm) under excitation at 633 nm. The merged image of VTAF and mitochondria mainly showed orange fluorescence signal (Figure 6), which indicates the fluorescence signal at two channels overlapped well. Quantitative image analysis showed a high Pearson's correlation coefficient of 0.86 ± 0.04

(detailed information on Pearson's correlation coefficient can be found in Supporting Information Figure S10).^{37,38} This results demonstrated that there are abundant VDPs in the mitochondria of live MCF-7 cells. As the key organelle for respiration, mitochondria are particularly susceptible to oxidative damage,^{39,40} and the mitochondrial VDPs may play a key role in both oxidative damage and redox signaling. These results were also consistent with previous report that abundant arsenic-binding proteins in MCF-7 cell lysate were mitochondrial related proteins.³⁴

Next, ratiometric fluorescence imaging of endogenous VDPs in live cells was also investigated. The ratio images were constructed from fluorescence signal of coumarin channel and naphthalimide channel by using ImageJ software. After the cells were treated with VTAF, the subcellular distribution of endogenous VDPs was observed through the emission ratio values (Figure 7, ratiometric image). The

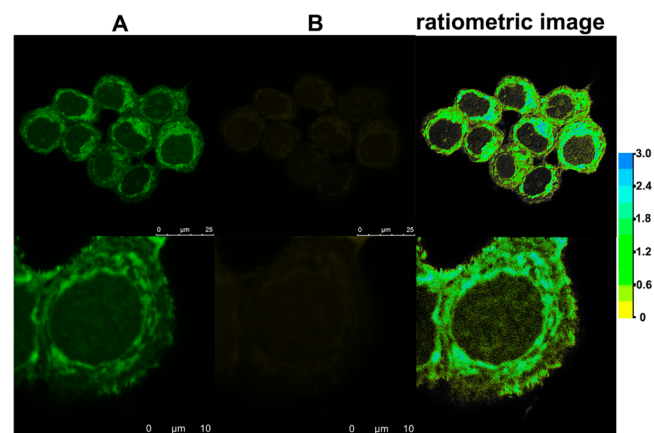


Figure 7. Ratiometric fluorescence imaging of endogenous VDPs with VTAF (5 μM) within live cells. Top: confocal ratiometric images of MCF-7 cells treated with VTAF. Scale bar 25 μm . Bottom: enlarged ratiometric image of single cells treated with VTAF. Scale bar 25 μm . (A) Fluorescence was collected at 450–490 nm (coumarin channel, left, green), (B) 530–590 nm (naphthalimide channel, middle, yellow) upon excitation by 405 nm laser line. Pseudocolor illustrates the ratio image generated from fluorescence intensities of coumarin channel to naphthalimide channel. Pseudocolor: yellow = low ratio, blue = high ratio.

cytoplasm matrix showed the emission ratio value of about 0.9. The punctuated patterns mainly concentrated in a small, eccentric perinuclear zone displayed emission ratio value of 2.7, which is 3-fold higher than ratio values in cytoplasm matrix. These results further confirmed that VTAF-labeled VDPs mainly localized in mitochondria. Meanwhile, ratio value of about 0.9 in cytoplasm matrix suggested low levels of VDPs were also present in cytoplasm matrix. Thus, the ratiometric images may enable a better understanding of subcellular distribution of endogenous VDPs through the direct readout of ratio values.

Flow Cytometric Analysis of VDPs in Suspension Cells with VTAF. Finally, we determined whether VTAF can be applied in flow cytometric analysis in tracing changes in levels of intracellular protein vicinal dithiols upon redox regulation in suspension cells. HL-60 cells (human promyelocytic leukemia cells) were loaded with VTAF (or VTAFc) and redox stimulants, respectively. Histograms showed the intracellular levels of vicinal dithiols on VDPs and

fluorescence signal from VTAF (or VTAFC) labeled VDPs was collected through a 450/50 band-pass filter with a total of 10^4 cells assessed (Figure 8 and Supporting Information

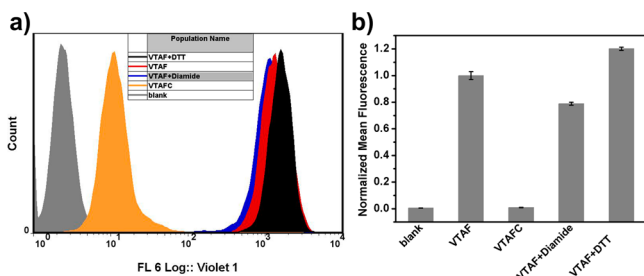


Figure 8. (a) Flow cytometric analysis of HL-60 cells loaded with VTAF and redox stimulants (10 mM DTT and 50 μ M Diamide). Violet 1 channel: 425–475 nm (450/50 band-pass filter). (b) Normalized mean fluorescence intensity per cell. Blank: HL-60 cells loaded without VTAF. VTAF, VTAFC, and VTAF + Diamide: cells loaded with VTAF, VTAFC, VTAF and Diamide, respectively. VTAF + DTT: cells loaded with VTAF first and incubation for 10 min, then DTT was loaded and incubation for another 20 min.

Figure S11). Compared to cells treated with VTAFC, a significant increase in fluorescence intensity was observed from the histogram of the VTAF-stained HL-60 cells (Figure 8a). In the case of cells loaded with VTAF and diamide, a decrease in the fluorescence intensity was observed. Similarly, the higher fluorescence intensity was observed in the VTAF and DTT treated cells (Figure 8a). Quantification of mean fluorescence intensity per cell clearly establishes a dynamic tracing in intracellular levels of proteins' vicinal dithiols under redox stimulus (Figure 8b). Notably, these results demonstrated that VTAF can be used in flow cytometry for simultaneous quantification of endogenous protein vicinal dithiols in HL60 cells. Hence, the VTAF-based flow cytometric analysis may present a new tool for the accurate evaluation of the roles of vicinal dithiols on VDPs against oxidative stress, which would be helpful for a better understanding of essential roles of protein vicinal dithiols in inflammation and cancer.

CONCLUSION

In summary, we have presented a ratiometric fluorescent probe (VTAF) for highly selective detection of endogenous protein vicinal dithiols in live cells for the first time. Compared to previous fluorescent probes for VDPs,^{25,26} VTAF embodies the quantitative determination of vicinal dithiols of VDPs through the readout of ratiometric fluorescence signal. Furthermore, VTAF was applied for specifically labeling cellular VDPs without washing procedures, which was beneficial for the in situ trapping of endogenous VDPs. In particular, the dynamic changes of cellular vicinal dithiols of VDPs can be traced by VTAF when the cells were stimulated by different redox reagents. The subcellular distribution of endogenous VDPs was clearly visualized in live cells through colocalization experiments and ratiometric images. This ratiometric fluorescent probe offers a noninvasive tools for collecting the global distribution and dynamic changes of endogenous VDPs in live cells, which may greatly contribute to further investigation on the essential roles of protein vicinal dithiols in cellular redox homeostasis and protein function in living cells. Through this approach, some

new endogenous redox-sensitive VDPs with diverse functions will also be unveiled, which can enable the discovery of promising new drug target for redox related diseases such as inflammation and cancers.

ASSOCIATED CONTENT

Supporting Information

Detailed experimental procedures and characterization of compounds. This material is available free of charge via the Internet at <http://pubs.acs.org>.

AUTHOR INFORMATION

Corresponding Authors

wpzhu@ecust.edu.cn

nqjia@shnu.edu.cn

yfxu@ecust.edu.cn

Notes

The authors declare no competing financial interest.

ACKNOWLEDGMENTS

We thank the financial support from National Natural Science Foundation of China (Grants 21476077, 21236002, 21373138, 21302125), National Basic Research Program of China (973 Program, 2013CB733700, 2010CB126100), National High Technology Research and Development Program of China (863 Program, 2011AA10A207), Shanghai Pujiang Program, Doctoral Fund of Ministry of Education of China (Grant No. 20133127120005), Program for Shanghai Sci. & Tech. Committee (Grants 13ZR1458800), Fundamental Research Funds for the Central Universities, Program for Cultivation of Young Teacher of Shanghai University.

REFERENCES

- (1) Maron, B. A.; Tang, S. S.; Loscalzo, J. *Antioxid. Redox Signaling* **2013**, *18*, 270–287.
- (2) Reddie, K. G.; Carroll, K. S. *Curr. Opin. Chem. Biol.* **2008**, *12*, 746–754.
- (3) Poole, L. B.; Nelson, K. J. *Curr. Opin. Chem. Biol.* **2008**, *12*, 18–24.
- (4) Ying, J.; Clavreul, N.; Sethuraman, M.; Adachi, T.; Cohen, R. A. *Free Radical Biol. Med.* **2007**, *43*, 1099–1108.
- (5) Valko, M.; Rhodes, C. J.; Moncol, J.; Izakovic, M.; Mazur, M. *Chem-Biol. Interact.* **2006**, *160*, 1–40.
- (6) Zhang, X.; Yan, X.; Zhou, Z.; Yang, F.; Wu, Z.; Sun, H.; Liang, W.; Song, A.; Lallemand-Breitenbach, V.; Jeanne, M.; Zhang, Q.; Yang, H.-Y.; Huang, Q.; Zhou, G.; Tong, J.; Zhang, Y.; Wu, J.; Hu, H.; de The, H.; Chen, S.; Chen, Z. *Science* **2010**, *328*, 240–243.
- (7) Houstis, N.; Rosen, E. D.; Lander, E. S. *Nature* **2006**, *440*, 944–948.
- (8) Sugatani, J.; Steinhilber, M. E.; Saito, K.; Olson, M. S.; Hanahan, D. J. *J. Biol. Chem.* **1987**, *262*, 16995–17001.
- (9) Matthias, L. J.; Hogg, P. J. *Antioxid. Redox Sign.* **2003**, *5*, 133–138.
- (10) Sahaf, B.; Heydari, K.; Herzenberg, L. A.; Herzenberg, L. A. *Arch. Biochem. Biophys.* **2005**, *434*, 26–32.
- (11) Ou, W.; Silver, J. *Virology* **2006**, *350*, 406–417.
- (12) Jain, S.; McGinnes, L. W.; Morrison, T. G. *J. Virol.* **2008**, *82*, 12039–12048.
- (13) Cook, K. M.; Hogg, P. J. *Antioxid. Redox Signaling* **2013**, *18*, 1987–2015.
- (14) Borges, C. R.; Lake, D. F. *Antioxid. Redox Signaling* **2014**, *21*, 392–395.
- (15) Walsh, C. T.; Garneau-Tsodikova, S.; Gatto, G. J. *Angew. Chem., Int. Ed.* **2005**, *44*, 7342–7372.

- (16) Gilbert, H. F. In *Methods in Enzymology*; Lester, P., Ed.; Academic Press: New York, 1995; Vol. 251, pp 8–28.
- (17) Bachi, A.; Dalle-Donne, I.; Scaloni, A. *Chem. Rev.* **2013**, *113*, 596–698.
- (18) Requejo, R.; Chouchani, E. T.; James, A. M.; Prime, T. A.; Lilley, K. S.; Fearnley, I. M.; Murphy, M. P. *Arch. Biochem. Biophys.* **2010**, *504*, 228–235.
- (19) Hoffman, R. D.; Lane, M. D. *J. Biol. Chem.* **1992**, *267*, 14005–14011.
- (20) Gitler, C.; Zarmi, B.; Kalef, E. *Anal. Biochem.* **1997**, *252*, 48–55.
- (21) McStay, G. P.; Clarke, S. J.; Halestrap, A. P. *Biochem. J.* **2002**, *367*, 541–548.
- (22) Moaddel, R.; Sharma, A.; Huseni, T.; Jones, G. S.; Hanson, R. N.; Loring, R. H. *Bioconjugate Chem.* **1999**, *10*, 629–637.
- (23) Heredia-Moya, J.; Kirk, K. L. *Biorg. Med. Chem.* **2008**, *16*, 5743–5746.
- (24) Turnbull, L.; Campbell, E. M.; Thomas, N. *Science* **2013**, *340*, 766.
- (25) Huang, C.; Yin, Q.; Zhu, W.; Yang, Y.; Wang, X.; Qian, X.; Xu, Y. *Angew. Chem., Int. Ed.* **2011**, *50*, 7551–7556.
- (26) Fu, N.; Su, D.; Cort, J. R.; Chen, B.; Xiong, Y.; Qian, W.-J.; Konopka, A. E.; Bigelow, D. J.; Squier, T. C. *J. Am. Chem. Soc.* **2013**, *135*, 3567–3575.
- (27) Whitney, M.; Savariar, E. N.; Friedman, B.; Levin, R. A.; Crisp, J. L.; Glasgow, H. L.; Lefkowitz, R.; Adams, S. R.; Steinbach, P.; Nashi, N.; Nguyen, Q. T.; Tsien, R. Y. *Angew. Chem., Int. Ed.* **2013**, *52*, 325–330.
- (28) Chang, C. J.; Jaworski, J.; Nolan, E. M.; Sheng, M.; Lippard, S. *J. Proc. Natl. Acad. Sci. U S A* **2004**, *101*, 1129–1134.
- (29) Zhou, X.; Su, F.; Lu, H.; Senechal-Willis, P.; Tian, Y.; Johnson, R. H.; Meldrum, D. R. *Biomaterials* **2012**, *33*, 171–180.
- (30) Fan, J.; Hu, M.; Zhan, P.; Peng, X. *Chem. Soc. Rev.* **2013**, *42*, 29–43.
- (31) Takakusa, H.; Kikuchi, K.; Urano, Y.; Sakamoto, S.; Yamaguchi, K.; Nagano, T. *J. Am. Chem. Soc.* **2002**, *124*, 1653–1657.
- (32) Zahler, W. L.; Cleland, W. W. *J. Biol. Chem.* **1968**, *243*, 716–719.
- (33) Huang, C.; Yin, Q.; Meng, J.; Zhu, W.; Yang, Y.; Qian, X.; Xu, Y. *Chem.—Eur. J.* **2013**, *19*, 7739–7747.
- (34) Zhang, X.; Yang, F.; Shim, J.-Y.; Kirk, K. L.; Anderson, D. E.; Chen, X. *Cancer Lett.* **2007**, *255*, 95–106.
- (35) Kosower, N. S.; Kosower, E. M.; Wertheim, B.; Correa, W. S. *Biochem. Biophys. Res. Commun.* **1969**, *37*, 593–596.
- (36) Donoghue, N.; Yam, P. T. W.; Jiang, X.-M.; Hogg, P. J. *Protein Sci.* **2000**, *9*, 2436–2445.
- (37) Adler, J.; Parmryd, I. *Cytometry, Part A* **2010**, *77*, 733–742.
- (38) French, A. P.; Mills, S.; Swarup, R.; Bennett, M. J.; Pridmore, T. P. *Nat. Protocols* **2008**, *3*, 619–628.
- (39) Murphy, M. P. *Biochem. J.* **2009**, *417*, 1–13.
- (40) Finkel, T. *Nat. Rev. Mol. Cell Biol.* **2005**, *6*, 971–976.